The Open Biotechnology Journal
DOI: 10.2174/0118740707449996260616050323, 2026, 20, e18740707449996
ISSN: 1874-0707
1

SHORT COMMUNICATION **OPEN ACCESS**

A Bio-Mimetic Approach: Non-adverse Effects of Zinc Oxide Nanoparticles with Probiotic Isolate (*Lactiplantibacillus plantarum*)

Kumar Vasuki[1], Balasubramanian Kaleeswaran[1,*] and Rengarajan Murugesan[2,*]

[1]*PG & Research Department of Zoology and Biotechnology, AVVM Sri Pushpam College (An Autonomous Institution, Affiliated to Bharathidasan University), Poondi, Thanjavur-613 503, Tamil Nadu, India*
[2]*Division of Entomology, Department of Bio Sciences, Rajagiri College of Social Sciences (An Autonomous Institution, Affiliated to Mahatma Gandhi University), Rajagiri P.O., Kalamassery, Cochin-683 104, Kerala, India*

Abstract:

Introduction: Green nanotechnology utilises biological systems to produce nanoparticles, offering environmentally friendly and sustainable alternatives to traditional chemical methods.

Methods: Biosynthesis of zinc oxide nanoparticles (ZnO NPs) using novel probiotic bacteria from the gut of the snail Pila globosa-derived probiotics (Lactiplantibacillus plantarum)-has promising applications in the development of health-related feed supplements. ZnO:LP NPs represent a significant advancement in the biomimetic approach for enhancing biocompatibility, structural uniformity, and antimicrobial effectiveness.

Results: Characterization of the synthesised nanoparticles, conducted using techniques such as Ultraviolet-Visible-Near Infrared (UV-Vis-NIR) spectroscopy, X-ray diffraction (XRD), Fourier Transform Infrared Spectroscopy (FTIR), Scanning Electron Microscopy (SEM), and Transmission Electron Microscopy (TEM), confirmed the successful formation of a hexagonal wurtzite structure. Biological assays were performed to investigate the synthesized nanoparticles, revealing significant antibacterial and cytotoxic activities.

Discussion: This research highlights the promising applications of probiotic nanoparticles.

Conclusion: This research highlights the potential of probiotic-based nanoparticles for the development of comprehensive feed supplements with nutraceutical and nutri-biotechnological applications, as well as their implications for the food and healthcare industries.

Keywords: Zinc oxide, Nanoparticles, *Lactiplantibacillus*, Feed supplement, Cytotoxicity.

*Address correspondence to these authors at the PG & Research Department of Zoology and Biotechnology, AVVM Sri Pushpam College (An Autonomous Institution, Affiliated to Bharathidasan University), Poondi, Thanjavur - 613 503, Tamil Nadu, India; E-mail: zookaleesh@gmail.com

Cite as: Vasuki K, Kaleeswaran B, Murugesan R. A Bio-Mimetic Approach: Non-adverse Effects of Zinc Oxide Nanoparticles with Probiotic Isolate (*Lactiplantibacillus plantarum*). Open Biotechnol J, 2026; 20: e18740707449996. http://dx.doi.org/10.2174/0118740707449996260616050323

Received: October 18, 2025
Revised: April 14, 2026
Accepted: April 21, 2026
Published: June 29, 2026

1. INTRODUCTION

Nanotechnology has emerged as an important field with applications in medicine, agriculture, food packaging, and environmental science. Among metal oxide nanoparticles, zinc oxide nanoparticles (ZnO NPs) have gained considerable attention due to their physicochemical stability and diverse biological activities [1]. Zinc is an essential trace element involved in numerous biological processes, and ZnO-based nanoparticles have been widely investigated for applications in environmental pollution control, cosmetics, agriculture, drug discovery, the textile industry, and biomedical applications [2]. However, due to

their increased surface area and biological reactivity compared to bulk zinc oxide, careful evaluation of their synthesis, characterization, and safety is necessary.

Green synthesis methods using biological systems offer environmentally friendly alternatives to conventional chemical approaches. Microorganisms can mediate nanoparticle formation through enzymatic reduction and biomolecule-assisted stabilization. Probiotic bacteria, particularly species belonging to the genera Lactobacillus, Bifidobacterium, Enterococcus, and Bacillus, have been widely studied for their beneficial health effects [3]. Among them, Lactiplantibacillus plantarum, a Gram-positive bacterium commonly used in food fermentation, produces bioactive metabolites such as proteins and organic acids that may function as reducing and stabilizing agents during nanoparticle synthesis [4].

Most commercially used probiotic strains are isolated from the human gastrointestinal tract or fermented foods [5]. In contrast, unconventional ecological niches may harbor probiotic microorganisms with distinct adaptive characteristics. The freshwater apple snail, Pila globosa, inhabits aquatic agricultural ecosystems and represents a relatively underexplored microbial reservoir. The isolation of probiotic strains from such environments may provide unique metabolic capabilities relevant to nanoparticle biosynthesis. Aquatic bacterial pathogens, including Aeromonas hydrophila, Escherichia coli, and Vibrio parahaemolyticus, contribute significantly to disease outbreaks in aquaculture systems. The growing concern about antimicrobial resistance underscores the need for alternative antimicrobial strategies. In this context, probiotic-mediated synthesis of ZnO nanoparticles may offer a biocompatible approach to developing antimicrobial agents. Therefore, the present study investigates the biosynthesis of ZnO nanoparticles using Lactiplantibacillus plantarum isolated from P. globosa, followed by detailed physicochemical characterization and evaluation of antibacterial activity against bacterial pathogens.

2. MATERIALS AND METHODS

2.1. Biosynthesis of Zinc Nanoparticle

Lactiplantibacillus plantarum was cultured in De Man, Rogosa, and Sharpe (MRS) broth at 37°C for 24 h under static conditions. The culture was centrifuged at 10,000 rpm for 15 min, and the supernatant was collected as cell-free supernatant (CFS). A 0.1 M zinc acetate dihydrate [$Zn(CH_3COO)_2 \cdot 2H_2O$] (Himedia, India; GRM692) solution was prepared using deionized water and used as the zinc precursor. The biosynthesis reaction was carried out by mixing CFS and zinc acetate solution in a 1:1 (v/v) ratio (50 mL each), giving a total reaction volume of 100 mL. The pH of the reaction mixture was measured using a calibrated digital pH meter and adjusted to 8.5-9.0 by the dropwise addition of 0.1 M sodium hydroxide (NaOH) under continuous magnetic stirring at 500 rpm. The reaction mixture was incubated at 80°C for 24 h with constant stirring, and nanoparticle formation was indicated by the development of white turbidity [3]. After incubation, the mixture was cooled to room temperature and centrifuged at 10,000 rpm for 15 min to collect the precipitate, which was washed three times with deionized water and ethanol to remove impurities. The product was dried at 60°C overnight and calcined at 400°C for 2 h to obtain zinc oxide nanoparticles (ZnONPs). The percentage yield was calculated using the formula (**1**):

$$\text{Yield (\%)} = \frac{\text{Weight of ZnONPs obtained}}{\text{Theoretical weight based on zinc precursor}} \text{X } 100 \quad \textbf{(1)}$$

Resulting in a final yield of 2.8 mg (approximately 70%). The synthesized nanoparticles were stored in an airtight container at room temperature under dry conditions for further use.

2.2. Characterisation Study

The crystallographic structure was examined using a powder X-ray diffraction (XRD) machine, specifically the D8 Advance ECO XRD system with an SSD160 1D detector, employing CuKα radiation (λ = 0.15406 nm). The FTIR (Fourier Transform Infrared Spectroscopy) spectrum was recorded on a Shimadzu IR-Trace 100 spectrometer. Perkin-Elmer LAMBDA-325 was used for optical analysis. To assess the surface morphology of the produced sample, a FE-SEM (Field Emission Scanning Electron Microscopy) was utilised, and the elemental composition was determined by recording the EDAX spectrum using the Carl Zeiss - Sigma 300 apparatus. The structural morphology of the synthesised material was analysed using a JEOL JEM-2100 HR-TEM (High-Resolution Transmission Electron Microscopy) instrument.

2.3. Antibacterial Activity

The antibacterial efficiency of probiotics must confer beneficial effects, and viable count generally assesses the effective probiotic dose at 1×10^8 CFU/mL, which is the minimum threshold for producing measurable biological and functional effects. For using concentration evaluated (**Supplementary Table 1**) by the agar well diffusion method against selected aquatic pathogens, including *Aeromonas hydrophila*, *Escherichia coli*, and *Vibrio parahaemolyticus*, at concentrations of 25, 50, 75, and 100 µg/mL. The plates were incubated at 37°C for 24 hrs, and the zone of inhibition was measured in each well, using sterile distilled water as a negative control to evaluate the results. As a positive control, 10 µg of amoxicillin was used. This experimental procedure was conducted in triplicate [6, 7].

2.4. Cytotoxicity Assay

The cytotoxicity of the ZnO: LP NPs was evaluated using the MTT assay [8]. The monolayer culture was trypsinized, and the cell count was adjusted to 1.0 × 10^5 cells/mL with complete culture medium containing 10% FBS. Cells were seeded at 1 × 10^4 cells/well in 96-well plates and incubated for 24 h to form a monolayer. The treatment solutions were then discarded, and 100 µL of MTT solution (0.5 mg/mL in PBS) was added to each well, followed by incubation for 4 h. The resulting formazan

crystals were dissolved by adding 100 µL of DMSO, and absorbance was measured at 590 nm using a microplate reader. Cell viability was expressed as a percentage relative to untreated control cells, and dose-response curves were used to assess cytotoxicity in L929 fibroblast cells.

2.5. Statistical Analysis

Statistical analysis has been added to evaluate the concentration-dependent antibacterial activity. Results are expressed as mean ± standard deviation, and statistical significance was assessed using one-way ANOVA with an appropriate post hoc test.

3. RESULTS AND DISCUSSION

The probiotic strain used in this study was isolated from the gut of *P. globosa*, a freshwater apple snail, which is an infrequent but potentially fruitful source of probiotic bacteria. Naturally suited to fluctuating aquatic conditions, snail-associated lactic acid bacteria (LAB) produce antibacterial metabolites, compete for colonization, and are stress-resistant. In this research, we synthesised ZnO nanoparticles using the isolated bacterial strain *Lactiplantibacillus plantarum* from *P. globosa*.

The XRD pattern (Fig. **1A**) shows sharp Bragg reflections at 2θ = 31.77° (100), 34.42° (002), 36.25 (101) °, 47.53° (102), 56.60° (110), 62.85° (103), 66.37° (200), 67.93° (112), and 69.03° (201), confirming the hexagonal wurtzite structure of ZnO (JCPDS Card No. 36-1451) [9]. The XRD data were collected over a 2θ range of 20°-80° with a step size of 0.02°. The prominent (100) peak intensity indicates preferred orientation, typical of biogenic ZnO from lactic acid bacteria due to anisotropic growth influenced by probiotic metabolites. Crystallite size was calculated using the Debye-Scherrer equation [10] and found to be 66 ± 5 nm, with an error representing instrumental and peak-broadening uncertainties formula (**2**).

$$D = \frac{K\lambda}{\beta \cos\theta} \quad \textbf{(2)}$$

Where K = 0.94 (spherical shape factor)

λ = 1.5406 Å (Cu Kα)

β = full width at half maximum (FWHM) = 0.21° (instrumentally corrected using Si standard)

Θ = 15.885° for the (100) peak

Yielding D = 66 nm

This size aligns with green-synthesised ZnO (50-80 nm), where probiotic capping limits excessive growth.

Uv-Vis-NIR spectroscopy (Fig. **1B**) reveals a broad absorption maximum at 337 nm, characteristic of ZnO excitonic transitions modified by quantum confinement and surface defect states. Spectra were recorded between 200 and 600 nm at 1 nm resolution in a 1 cm quartz cuvette, using deionised water as a blank. Baseline correction was performed by two-point subtraction in OriginPro 2023 (linear fit, R^2 > 0.999). The broad, monotonic profile (no sharp excitonic peak) reflects polydisperse nanograins capped with oxygen vacancies (Vo) and zinc interstitials (Zni) from *L. plantarum*, consistent with reports of probiotic ZnO.

The optical band gap energy was determined using Tauc's relation for direct-allowed transitions formula (**3**) (Fig. **1C**).

$$(\alpha h\nu)^2 = B\,(h\nu - E_g) \quad \textbf{(3)}$$

Where the absorption coefficient $\alpha = \frac{2.303\,A}{d}$

(A= absorbance, d= 1 cm path length)

$h\nu$ is Photon energy, and B is the edge parameter.

The linear fitting was performed in the photon energy range of 2.6-3.2 eV (R^2 = 0.992). Extrapolation of the linear portion to the energy axis yielded a band gap value of 2.9 eV. The slight red-shift compared to bulk ZnO (3.2-3.37 eV) is attributed to defect-induced mid-gap states, particularly oxygen vacancy (V_o) donor levels located approximately 0.2-0.5 eV below the conduction band. These defect states and surface interactions introduced during synthesis contribute to band gap narrowing. The R^2 value confirms that the fitting excluded Urbach tail contributions, ensuring reliable estimation in accordance with established ZnO optical analysis protocols [11-13].

Bacterial supernatant reveals key functional groups involved in reduction and stabilisation. Peaks around 3300-3400 cm^{-1} correspond to O-H stretching from hydroxyl groups, 1650 cm^{-1} and 1540 cm^{-1} represent amide I and II bands, indicating the presence of proteins or peptides, and the sharp peak at 450-500 cm^{-1} confirms the formation of Zn-O bonds (Fig. **1D**). Similarly, Ezealisiji *et al*. [14] demonstrated the synthesis of microorganism-based ZnO nanoparticles with an absorption peak at 359 nm. FTIR spectra (KBr pellet, 400-4000 cm^{-1} resolution, post-400°C calcination (2h, air atmosphere) confirm partial retention of bioactive capping. Table **1** provides quantitative peak assignments and retention efficiencies (calculated from pre- and post-calcination peak area ratios).

Table 1. FTIR spectra quantitative peak assignments.

Wavenumber (cm^{-1})	Assignment	Origin (*L. plantarum*)	Post-Calcination Retention
3300-3400	O-H stretching (H-bonded)	Hydroxyls, residual water	85%
1650	Amide I (C=O stretch)	Peptide carbonyls (capping)	70%
1540	Amide II (N-H bend)	Protein secondary structure	65%
450-500	Zn-O lattice vibration	Wurtzite ZnO core	100% (sharpened)

Calcination at 400°C selectively decomposes labile organics while preserving thermostable peptide/proteins (decomposition >500°C), enhancing crystallinity without complete capping loss. This is evidenced by sustained amide bands matching those of *L. plantarum*-ZnO and unchanged MIC/MBC values, indicating retention of bioactivity. Our results are consistent with those reported by Mohd Yusof *et al*. [3], who found that ZnO-based *Lactiplantibacillus plantarum* nanoparticles exhibited an absorption peak at 3273.8 cm^{-1}, indicating the presence of hydroxyl functional groups. Agglomerated ZnO nanograin clusters, which are frequently seen in biologically produced nanoparticles following calcination due to the elimination of organic stabilizing macromolecules, were revealed by SEM and TEM investigations. SEM micrographs (Fig. **1E**), obtained at an accelerating voltage of 5 kV (200 nm resolution), reveal agglomerated nanograins (20-70 nm range), with a mean diameter of 49 nm (n=100 particles). These synthesised nanograins were exhibited. TEM analysis (Fig. **1F**) performed at an accelerating voltage of 200 kV confirms primary crystallites (~49 nm, n=200 particles) within fractal-like aggregates (mean=48.5 nm, Gaussian fit SD=12.3 nm; histogram, Fig. **1G**). Aggregation arises from weakened van der Waals forces after calcination of the probiotic capping, but modulates bioactivity favourably: clusters slow Zn^{2+} dissolution and the ROS burst, reducing cytotoxicity while sustaining membrane disruption. EDX mapping (Fig. **1H**) confirms the elemental stoichiometry: Zn (63%), O (32%), and C (5%) with an atomic ratio Zn:O ≈ 1:1.2, consistent with surface hydroxylation.

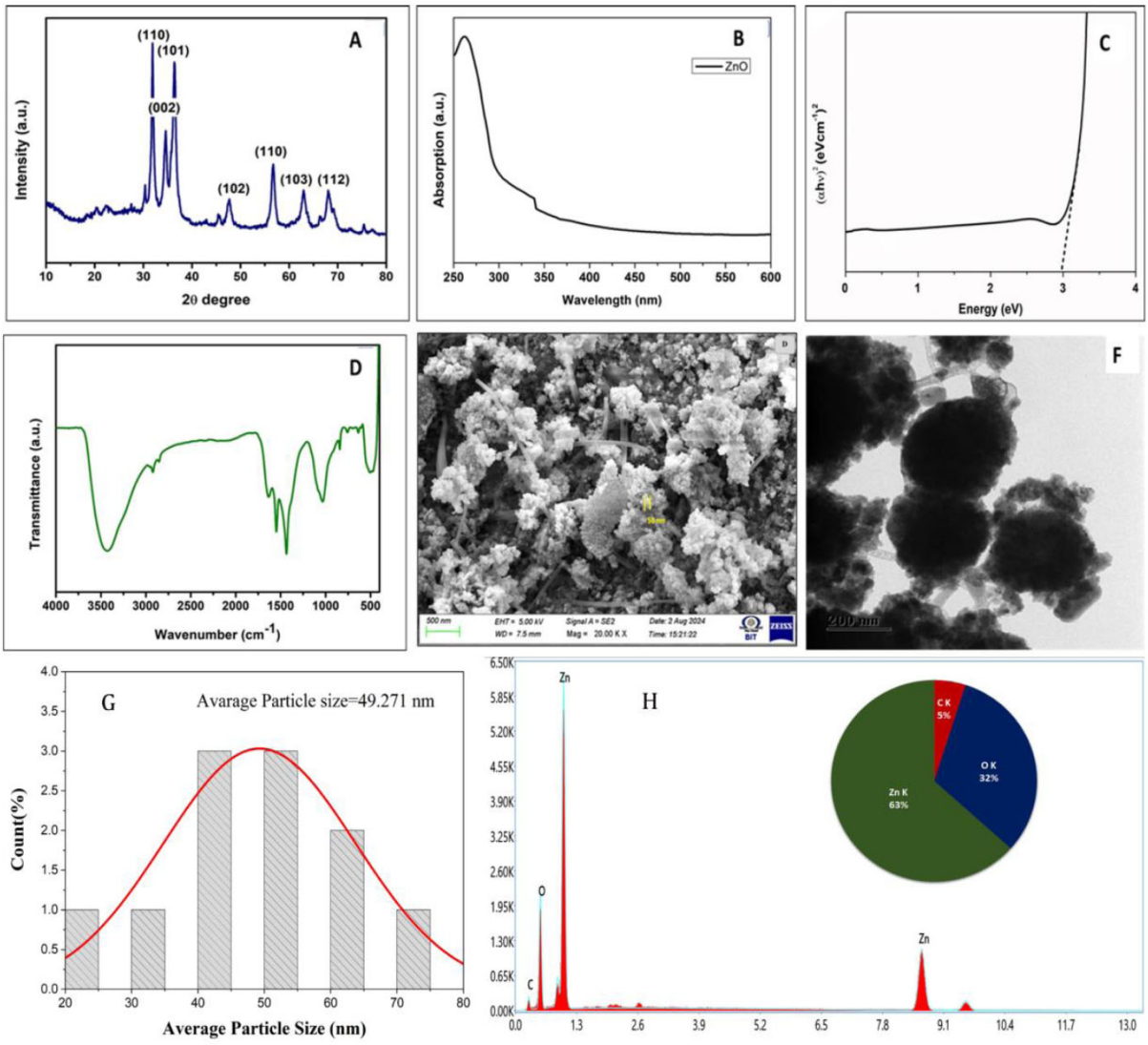

Fig. (1). Confirmation and characterization images of synthesized ZnO: LP NPs.
(**A**) XRD pattern; (**B**) UV-Vis Spectrum; (**C**) Tauc's plot;D) FTIR pattern; (**E**) SEM; (**F**) TEM; (**G**) EDX; (**H**) Particle Size.

Characterization of Synthesized ZnO nanoparticle-based *Lactiplantibacillus plantarum*

3.1. Anti-bacterial Activity of ZnO-based *Lactiplantibacillus plantarum*

The antibacterial activity of ZnO: LP NPs was evaluated against the three pathogens *A. hydrophila*, *E. coli*, and *V. parahaemolyticus* using the agar well diffusion method. Fresh overnight bacterial cultures were adjusted to the 0.5 McFarland standard (approximately 1×10^8 CFU/mL) and uniformly swabbed onto sterile Muller-Hinton agar plates. Wells of 6 mm diameter were aseptically punched into the agar and loaded with ZnO: LP NPs suspensions at concentrations of 25, 50, 75, and 100 µg/mL (Fig. **2**). Sterile distilled water served as the negative control to ensure that inhibition was not due to solvent effects. The plates were incubated at 37°C for 24 h, after which the zones of inhibition were measured in millimetres. The positive control (Amoxicillin) has been included. The zone of inhibition values is: *A. hydrophila* (3.005 ± 0.004 mm), *E. coli* (3.572 ± 0.012 mm), *and V. parahaemolyticus* (3.274 ± 0.027 mm). All experiments were conducted in triplicate, and results were expressed as mean ± standard error.

To determine the minimum inhibitory concentration (MIC) and minimum bactericidal concentration (MBC), both assays were performed according to CLSI guidelines. Twofold serial dilutions of ZnO: LP NPs (12.5 µg/mL-100 µg/mL) were prepared in Muller-Hinton broth and inoculated with bacteria suspensions adjusted to approximately 1×10^6 CFU/mL. After incubation at 37°C for 24 h, the MIC (expressed in µg/mL) was defined as the lowest concentration of ZnO: LP NPs that inhibited visible bacterial growth. Aliquots from wells showing no visible growth were subcultured onto fresh Muller-Hinton agar plates and incubated for 24 h. MBC (expressed in µg/mL) was defined as the lowest concentration resulting in complete absence of colony formation (≥99.9% bacterial killing) (Table **2**).

Table 2. Antibacterial activity of ZnO: LP NPs and control treatments against selected aquatic pathogens.

Test Organism	Treatment	Zone of Inhibition (mm)	MIC (µg/mL)	MBC (µg/mL)
Aeromonas hydrophila	ZnO: LP NPs (25 µg/mL)	0.866 ± 0.033	25	50
	ZnO: LP NPs (50 µg/mL)	1.200 ± 0.057	-	-
	ZnO: LP NPs (75 µg/mL)	1.533 ± 0.088	-	-
	ZnO: LP NPs (100 µg/mL)	1.800 ± 0.057	-	-
	Ciprofloxacin (10 µg/disc)	3.500 ± 0.120	ND	ND
	Cell-free supernatant	0.200 ± 0.015	ND	ND
	Zinc acetate solution	0.150 ± 0.020	ND	ND
	Amoxicillin positive control	3.005 ± 0.004	ND	ND
	Negative control (DW)	No inhibition	ND	ND
Escherichia coli	ZnO: LP NPs (25 µg/mL)	0.466 ± 0.033	25	50
	ZnO: LP NPs (50 µg/mL)	0.700 ± 0.057	-	-
	ZnO: LP NPs (75 µg/mL)	0.966 ± 0.088	-	-
	ZnO: LP NPs (100 µg/mL)	1.333 ± 0.120	-	-
	Ciprofloxacin (10 µg/disc)	3.200 ± 0.105	ND	ND
	Cell-free supernatant	0.150 ± 0.018	ND	ND
	Zinc acetate solution	0.120 ± 0.016	ND	ND
	Amoxicillin positive control	3.572 ± 0.012	ND	ND
	Negative control (DW)	No inhibition	ND	ND
Vibrio parahaemolyticus	ZnO: LP NPs (25 µg/mL)	0.400 ± 0.057	25	50
	ZnO: LP NPs (50 µg/mL)	0.600 ± 0.057	-	-
	ZnO: LP NPs (75 µg/mL)	0.833 ± 0.176	-	-
	ZnO: LP NPs (100 µg/mL)	1.266 ± 0.088	-	-
	Ciprofloxacin (10 µg/disc)	3.000 ± 0.098	ND	ND
	Cell-free supernatant	0.180 ± 0.020	ND	ND
	Zinc acetate solution	0.140 ± 0.019	ND	ND
	Amoxicillin positive control	3.274 ± 0.027	ND	ND
	Negative control (DW)	No inhibition	ND	ND

Note: Values represent Mean ± SE (n = 3). MIC: Minimum Inhibitory Concentration determined by the broth microdilution method. MBC: Minimum Bactericidal Concentration determined by the sub-culturing method. ND: Not determined. DW: Distilled Water.

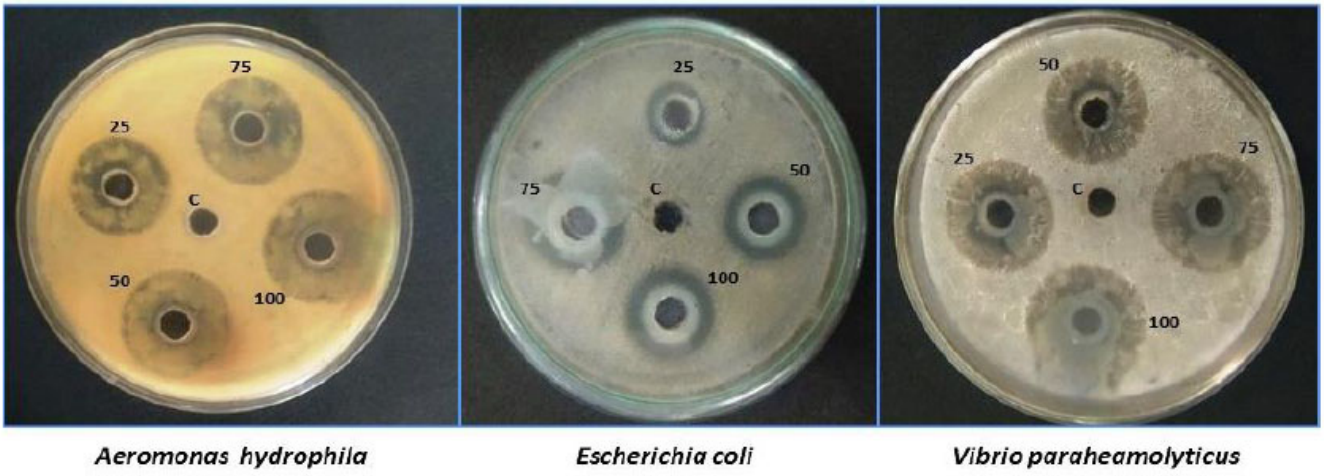

Fig. (2). Antibacterial activity of ZnO: LP NPs at different concentrations (25, 50, 75, and 100 µg/mL).

To confirm that the antibacterial activity was specifically attributable to the synthesized ZnO NPs, appropriate controls were included. The sterile cell-free supernatant from a *L. plantarum* culture (without a zinc precursor) was tested separately to evaluate the contribution of probiotic metabolites, and only minimal inhibition was observed. Similarly, zinc acetate solution at equivalent concentrations was tested independently and showed negligible antibacterial activity compared to ZnO: LP NPs. These control experiments demonstrate that the observed antibacterial effect primarily resulted from the synthesized ZnO NPs rather than residual bacterial metabolites or unreacted zinc precursor. The concentration-dependent increase in inhibition zones, along with MIC (25 µg/mL) and MBC (50 µg/mL) values, confirms the effective bacteriostatic and bactericidal properties of the ZnO: LP NPs formulation. According to Rajivgandhi *et al*. [15], biosynthesized ZnO nanoparticles were more effective against *S. aureus* than against *E. coli*, a trend also observed in our studies. Khatami *et al*. [16] reported that biosynthesized ZnO nanoparticles demonstrated enhanced inhibitory activity against both *S. aureus* and *E. coli*, with MIC and MBC values of 20.0 µg/mL. This activity is likely due to bacteriocins and organic acids produced by the probiotic strain, underscoring the formulation's dual role in pathogen control. Such properties are particularly beneficial for enhancing biosecurity in aquaculture and offer potential applications in food safety and human health.

3.2. Cytotoxicity Assay

The calculated IC_{50} value was 38.75 µg/mL, indicating moderate cytotoxicity. At concentrations ≤20 µg/mL, cell viability remained above 40%, demonstrating partial cytocompatibility at lower doses (Fig. **3AC**). However, a pronounced dose-dependent decline in viability was observed at concentrations above 30 µg/mL, with complete inhibition occurring at 50 µg/mL and higher [17, 18]. These findings suggest that the cellular response is strongly concentration-dependent and highlight the importance of dose optimization in potential applications.

Numerous *in vitro* studies have shown that ZnO nanoparticles may pose risks to various cell types [14]. Notable harmful effects include the induction of oxidative stress and cellular damage associated with the release of free Zn^{2+} ions from ZnO nanoparticles, leading to cellular injury. Nevertheless, findings regarding the cytotoxic effects of ZnO nanoparticles on cell lines are not always consistent. According to Fouda *et al*. [19], nanoparticle cytotoxicity is influenced by factors such as size, shape, and dosage. This aligns with earlier findings showing that ZnO-NPs exhibit selective cytotoxicity depending on size, surface charge, and capping agents. Hypothetically, ZnO nanoparticles release Zn^{2+} ions and generate reactive oxygen species (ROS), leading to oxidative stress, membrane and cellular disruption, mitochondrial dysfunction, and DNA damage, resulting in bacterial cell death or eukaryotic cell apoptosis [1]. However, the biosynthesis of probiotic-mediated ZnO nanoparticles involves biomolecule-assisted nucleation, biological capping, and controlled growth, resulting in nanoparticles that exhibit enhanced antibacterial effects through ROS generation and membrane disruption while maintaining dose-dependent biocompatibility in mammalian cells. Future studies should incorporate complementary assays, such as intracellular ROS quantification, caspase activation analysis, membrane integrity assays (*e.g.*, LDH release), mitochondrial membrane potential measurements, and evaluation of apoptosis markers, to provide a more comprehensive assessment of nanoparticle-induced cellular responses. Furthermore, although probiotic-mediated synthesis may influence nanoparticle growth and surface characteristics during formation, calcination at elevated temperatures likely reduces the persistence of surface biomolecules. Therefore, the nanoparticles produced in this study are best described as biologically initiated rather than definitively biologically capped after calcination.

3A

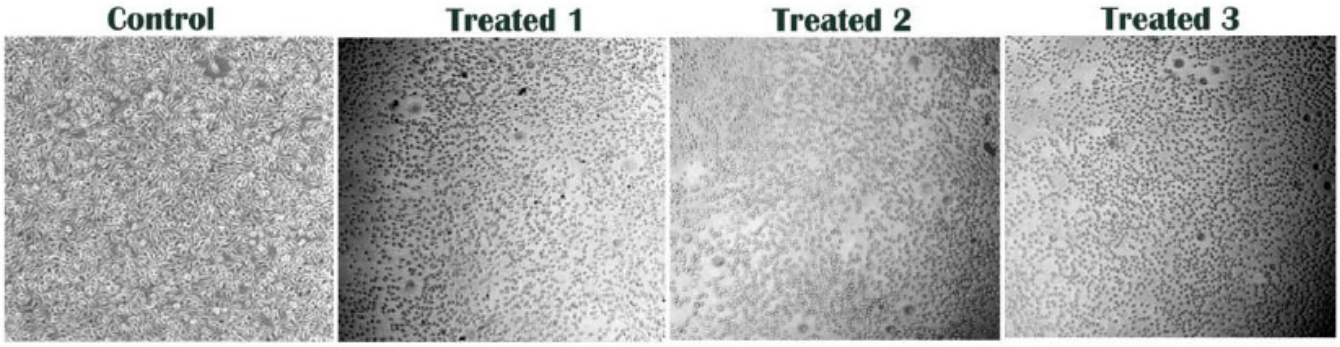

3B

Concentration (µg/mL)	% Cell Viability (mean ± SD)
0	100 ± 0.3
10	71.9 ± 0.4
20	43.9 ± 0.2
30	20.8 ± 0.3
40	3.8 ± 0.2

3C

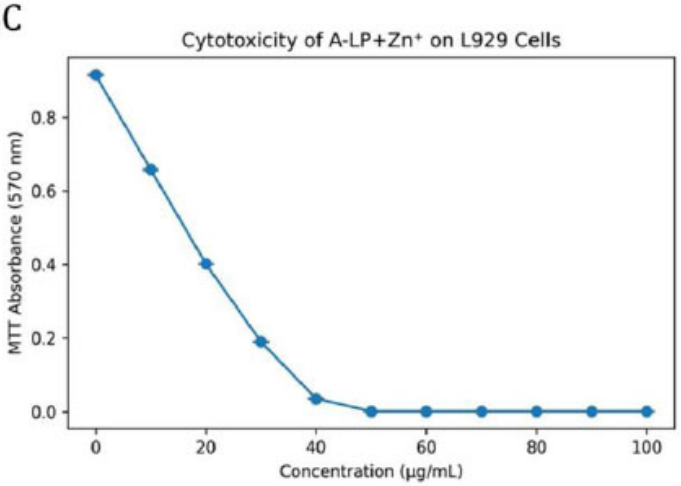

Fig. (3). Cytotoxicity and cell viability of the L929 fibroblast cell line. **A**: Micrograph of the cell line; **B**: Cell viability (%); **C**: IC_{50} value against dose-response at concentrations (µg/mL).

CONCLUSION

The isolated probiotic bacterium *L. plantarum* was found to be an effective and environmentally acceptable biocatalyst for the biosynthesis of ZnO NPs, producing nanoscale particles with confirmed structural characteristics and concentration-dependent antibacterial activity. The distinctive metabolic profile of this probiotic likely contributed to the stability and bioactivity of the synthesized nanoparticles. The ZnO: LP NPs demonstrated measurable antibacterial effects against aquatic pathogens, with controlled dose-dependent cytotoxic responses observed in L929 fibroblast cells. The findings highlight the potential of probiotic-mediated ZnO NPs for antimicrobial applications in aquaculture and related systems. Further studies, including *in vivo* evaluation and long-term safety assessment, are necessary to validate their broader biomedical applicability.

AUTHORS' CONTRIBUTIONS

The authors confirm contribution to the paper as follows: K.V.: Contributed to writing the original draft, methodology, and data collection; B.K.: Contributed to writing the original draft, writing review and editing, software, and methodology; R.M.: Contributed to writing the original draft, writing review and editing, software, and methodology. All authors reviewed the results and approved the final version of the manuscript.

LIST OF ABBREVIATIONS

CFS	=	Cell-Free Supernatant
FTIR	=	Fourier transform Infrared Spectroscopy
LAB	=	Lactic Acid Bacteria
NaOH	=	Sodium Hydroxide
NPs	=	Nanoparticles
SEM	=	Scanning Electron Microscopy
UV-Vis-NIR	=	Ultraviolet-Visible-Near Infrared
XRD	=	X-ray diffraction
ZnO	=	Zinc Oxide Nanoparticles

ETHICS APPROVAL AND CONSENT TO PARTICIPATE

Not applicable.

HUMAN AND ANIMAL RIGHTS

Not applicable.

CONSENT FOR PUBLICATION

Not applicable.

AVAILABILITY OF DATA AND MATERIALS

The data and supportive information is available within the article.

FUNDING

None.

CONFLICT OF INTEREST

Rengarajan Murugesan is the Associate Editorial Board Member of the journal TOBIOTJ.

ACKNOWLEDGEMENTS

All authors acknowledge and thank their institution for moral support of this research.

SUPPLEMENTARY MATERIAL

Supplementary material is available on the publisher's website along with the published article.

REFERENCES

[1] Sirelkhatim A, Mahmud S, Seeni A, *et al*. Review on Zinc Oxide nanoparticles: Antibacterial activity and toxicity mechanism. Nano-Micro Lett 2015; 7(3): 219-42. http://dx.doi.org/10.1007/s40820-015-0040-x PMID: 30464967

[2] Raha S, Ahmaruzzaman M. ZnO nanostructured materials and their potential applications: Progress, challenges and perspectives. Nanoscale Adv 2022; 4(8): 1868-925. http://dx.doi.org/10.1039/D1NA00880C PMID: 36133407

[3] Mohd Yusof H, Mohamad R, Zaidan UH, Rahman NAA. Sustainable microbial cell nanofactory for zinc oxide nanoparticles production by zinc-tolerant probiotic *Lactobacillus plantarum* strain TA4. Microb Cell Fact 2020; 19(1): 10. http://dx.doi.org/10.1186/s12934-020-1279-6 PMID: 31941498

[4] Chakra PS, Banakar A, Puranik SN, Kaveeshwar V, Ravikumar CR, Gayathri D. Characterization of ZnO nanoparticles synthesized using probiotic *Lactiplantibacillus plantarum* GP258. Beilstein J Nanotechnol 2025; 16: 78-89. http://dx.doi.org/10.3762/bjnano.16.8 PMID: 39902341

[5] Hill C, Guarner F, Reid G, *et al*. The International Scientific Association for Probiotics and Prebiotics consensus statement on the scope and appropriate use of the term probiotic. Nat Rev Gastroenterol Hepatol 2014; 11(8): 506-14. http://dx.doi.org/10.1038/nrgastro.2014.66 PMID: 24912386

[6] Parihar J, Kumawat A, Misra KP, Bagaria A. Extracellular synthesis of Zinc Oxide nanoparticles using thermo-halotolerant aeribacillus pallidus strain SJP 27: Characterization and antibacterial potential. J Nano Electronic Physics 2021; 13(2) http://dx.doi.org/10.21272/jnep.13(2).02007

[7] Santhoshkumar J, Kumar SV, Rajeshkumar S. Synthesis of zinc oxide nanoparticles using plant leaf extract against urinary tract infection pathogen. Resour.-. Effic Technol 2017; 3: 459-65.

[8] Singh P, Kim YJ, Zhang D, Yang DC. Biological Synthesis of Nanoparticles from Plants and Microorganisms. Trends Biotechnol 2016; 34(7): 588-99. http://dx.doi.org/10.1016/j.tibtech.2016.02.006 PMID: 26944794

[9] Ravichandran K, Chidhambaram N, Gobalakrishnan S. Copper and Graphene activated ZnO nanopowders for enhanced photocatalytic and antibacterial activities. J Phys Chem Solids 2016; 93: 82-90. http://dx.doi.org/10.1016/j.jpcs.2016.02.013

[10] Holzwarth U, Gibson N. The Scherrer equation *versus* the 'Debye-Scherrer equation'. Nat Nanotechnol 2011; 6(9): 534-4. http://dx.doi.org/10.1038/nnano.2011.145 PMID: 21873991

[11] Gharpure S, Yadwade R, Ankamwar B. Non-antimicrobial and non-anticancer properties of ZnO nanoparticles biosynthesized using different plant parts of *Bixa orellana*. ACS Omega 2022; 7(2): 1914-33. http://dx.doi.org/10.1021/acsomega.1c05324 PMID: 35071882

[12] Coulter JB, Birnie DP III. Assessing Tauc Plot Slope quantification: ZnO thin films as a model system. Phys Status Solidi, B Basic Res 2018; 255(3): 1700393. http://dx.doi.org/10.1002/pssb.201700393

[13] Sáenz-Trevizo A, Amézaga-Madrid P, Pizá-Ruiz P, Antúnez-Flores W, Miki-Yoshida M. Optical Band Gap estimation of ZnO Nanorods. Mater Res 2016; 19: 33-8. http://dx.doi.org/10.1590/1980-5373-mr-2015-0612

[14] Ezealisiji KM, Siwe-Noundou X, Maduelosi B, Nwachukwu N, Krause RWM. Green synthesis of zinc oxide nanoparticles using *Solanum torvum (L)* leaf extract and evaluation of the toxicological profile of the ZnO nanoparticles-hydrogel composite in Wistar albino rats. Int Nano Lett 2019; 9(2): 99-107. http://dx.doi.org/10.1007/s40089-018-0263-1

[15] Rajivgandhi G, Ramachandran G, Maruthupandy M, Manoharan N, Quero F. Biosyntheis of zinc oxide nanoparticles using Lactobacillus plantarum TA4 and its antibacterial and biocompatibility studies. Sci Rep 2020; 10: 19184. http://dx.doi.org/10.1038/s41598-020-76402-w

[16] Khatami M, Alijani HQ, Heli H, Sharifi I. Rectangular shaped zinc oxide nanoparticles: Green synthesis by Stevia and its biomedical efficiency. Ceram Int 2018; 44(13): 15596-602. http://dx.doi.org/10.1016/j.ceramint.2018.05.224

[17] Mushtaq S, Shahzad K, Saeed T, *et al*. Biocompatibility and cytotoxicity *in vitro* of surface-functionalized drug-loaded spinel ferrite nanoparticles. Beilstein J Nanotechnol 2021; 12: 1339-64. http://dx.doi.org/10.3762/bjnano.12.99 PMID: 34934608

[18] Bukar AM, Abdullah Jesse FF, Che Abdullah CA, *et al*. *In vitro* cytotoxicity evaluation of green synthesized alumina nanoscales on different mammalian cell lines. Sci Rep 2024; 14(1): 22826. http://dx.doi.org/10.1038/s41598-024-53204-y PMID: 39353973

[19] Fouda A, EL-Din Hassan S, Salem SS, Shaheen TI. *In-Vitro* cytotoxicity, antibacterial, and UV protection properties of the biosynthesized Zinc oxide nanoparticles for medical textile applications. Microb Pathog 2018; 125: 252-61. http://dx.doi.org/10.1016/j.micpath.2018.09.030 PMID: 30240818